Journal of Organometallic Chemistry, 410 (1991) 85–99
Elsevier Sequoia S.A., Lausanne
JOM 21713

Reactions of the triosmium complex $Os_3(CO)_{10}(\mu\text{-Br})(CH{=}CHPh)$ with benzyl isonitrile and triphenylphosphine. Crystal structure and solution fluxionality of the ethenyl derivatives

Shiow-Huey Chuang, Yun Chi *, Fen-Ling Liao, Sue-Lein Wang
Department of Chemistry, National Tsing Hua University, Hsinchu 30043 (Taiwan)

Shie-Ming Peng, Gene-Hsiang Lee
Department of Chemistry, National Taiwan University, Taipei 10764 (Taiwan)

Jung-Chung Wu and Keh-Ming Horng
Refining and Manufacturing Research Center, CPC, Chiayi 60036 (Taiwan)

(Received December 7th, 1990)

Abstract

Reaction of $Os_3(CO)_{10}(\mu\text{-Br})(CH{=}CHPh)$ (**1**) with benzyl isonitrile in toluene at 85°C gave a trinuclear complex $Os_3(CO)_9(CNCH_2Ph)(\mu\text{-Br})(CH{=}CHPh)$ (**2**). In contrast, the analogous reaction with triphenylphosphine at 110°C produced dinuclear complexes $Os_2(CO)_5(PPh_3)(\mu\text{-Br})(CH{=}CHPh)$ (**4**). The ethenyl group of complex **2** is static; however, variable temperature NMR studies indicate that the ethenyl groups of **3** and **4** undergo rapid $\pi \rightarrow \sigma, \sigma \rightarrow \pi$ rearrangement (reversible flipping of the vinyl group) in solution. The structures of **2** and **3** were also determined by single-crystal X-ray diffraction. Crystal data for **2**: space group $P2_1/c$; $a = 9.977(2)$, $b = 22.779(6)$, $c = 25.323(5)$ Å, $\beta = 95.08(2)°$, $Z = 8$; final $R = 0.038$, $R_w = 0.037$ for 3445 reflections with $I \geq 3\sigma(I)$. Crystal data for **3**: space group $P\bar{1}$; $a = 10.749(2)$, $b = 13.101(3)$, $c = 13.208(3)$ Å, $\alpha = 118.73(2)$, $\beta = 105.4992)$, $\gamma = 97.62(2)°$; $Z = 2$; final $R = 0.027$, $R_w = 0.026$ for 4211 reflections with $I > 2\sigma(I)$.

Introduction

The addition of anionic nucleophiles, such as halide anions, is used routinely in the chemical industry to improve the activity, selectivity and stability of transition metal catalysts [1]. However, the influence of the promoter on the bonding and reactivity of adsorbed hydrocarbon ligands is poorly understood at present [2], but there is increasing research activity on related subjects. The halide-promoted insertion of carbon monoxide into the bridging methylene group of the anionic triosmium clusters has been reported [3]. Recent work has considered the halide-promoted reactions of alkynes with $Ru_3(CO)_{12}$ [4] a halogen induced cluster fragmenta-

0022-328X/91/$03.50

tion of a carboxamide-substituted triosmium complex has been found [3]. These investigations have underlined the progress in the study of the chemistry of halogens in transition metal complexes.

With a similar objective, to probe the influence of halogen atoms on the adjacent hydrocarbon fragment in the coordination sphere of cluster complexes, we synthesized a triosmium ethenyl complex $Os_3(CO)_{10}(\mu\text{-Br})(CH{=}CHPh)$ (**1**) from the reaction of $H_2Os_3(CO)_{10}$ and phenylbromoethyne, and explored its CO elimination, hydrogenation and dehydrogenation reactions in attempts to compare its reactivity with that of the triosmium hydrido analogue $Os_3(CO)_{10}(\mu\text{-H})(CH{=}CHPh)$ [6]. In the present paper, we report the reactions of **1** with two nucleophiles, namely triphenylphosphine and benzyl isonitrile. Our results reveal that the reaction with benzyl isonitrile led to a simple substitution product $Os_3(CO)_9(CNCH_2Ph)(\mu\text{-Br})(CH{=}CHPh)$ (**2**), but the reaction with triphenylphosphine afforded a cluster fragmentation product $Os_2(CO)_5(PPh_3)(\mu\text{-Br})(CH{=}CHPh)$ (**3**). The complex **3** also reacted with triphenylphosphine to yield $Os_2(CO)_4(PPh_3)_2(\mu\text{-Br})(CH{=}CHPh)$ (**4**) under the reaction conditions examined. In addition, the ethenyl ligand of **3** and **4** undergoes a rapid $\pi \rightarrow \sigma,\sigma \rightarrow \pi$ rearrangement [7] (vinyl group flipping) in solution, as indicated by variable temperature ^1H and ^{13}C NMR studies.

Experimental

General information and materials

Infrared spectra were recorded on a Bomen M-100 FT-IR spectrometer. ^1H and ^{13}C NMR spectra were recorded on a Bruker AM-400 (400.13 MHz) instrument or a Varian Gemini-300 (300 MHz) instrument. Mass spectra were obtained on a JEOL-HX110 instrument operating in the fast atom bombardment mode (FAB). All reactions were performed under a nitrogen atmosphere using deoxygenated solvents dried with an appropriate reagent. The progress of reactions was monitored by analytical thin-layer chromatography (5735 Kieselgel 60 F_{254}, E. Merck) and the products were separated on preparative thin-layer chromatographic plates (Kieselgel 60 F_{254}, E. Merck). Elemental analyses were performed at the NSC Regional Instrumentation Center at National Cheng Kung University, Tainan, Taiwan. The triosmium complex $Os_3(CO)_{10}(\mu\text{-Br})(CH{=}CHPh)$ (**1**) was prepared according to a previously published procedure [6]. The ^{13}CO enriched sample of **1** was prepared by reaction of phenylbromoethyne with ^{13}CO enriched $H_2Os_3(CO)_{10}$ under similar conditions.

Reaction of $Os_3(CO)_{10}(\mu\text{-Br})(CH{=}CHPh)$ with benzyl isonitrile

A toluene solution (35 mL) of a mixture of $Os_3(CO)_{10}(\mu\text{-Br})(CH{=}CHPh)$ (134 mg, 0.13 mmol) and 1.3 equiv. of benzyl isonitrile (19.7 μL, 0.17 mmol) was heated at 85 °C for 30 min. Then the solvent was evaporated on a rotary evaporator, and the residue separated by thin layer chromatography (dichloromethane : hexane = 1 : 3), giving 51.8 mg of $Os_3(CO)_9(CNCH_2Ph)(\mu\text{-Br})(CH{=}CHPh)$ (**2**), as an orange crystalline material (0.046 mmol, 36%). Crystals of **2** suitable for X-ray diffraction were obtained by recrystallization from a layered solution of dichloromethane–methanol at room temperature.

Spectroscopic data for **2**: MS (FAB, ^{79}Br, ^{192}Os), m/z 1127 (M^+). IR (C_6H_{12}): ν(CN), 2184br,w; ν(CO), 2085s, 2067vw, 2050s, 2028s, 2018m, 2000vs, 1988m,

1982w, 1971w, 1964w cm^{-1}; ^1H NMR (400 MHz, $CDCl_3$, 294K): δ 7.40–7.12 (m, 10H); 6.99 (d, 1H, J(H–H) = 16.0 Hz); 5.92 (d, 1H, J(H–H) = 16.0 Hz); 5.07 (d, 1H, J(H–H) = 16.7 Hz), 5.00 (d, 1H, J(H–H) = 16.7 Hz). Elemental analysis: Found: C, 26.78; H, 1.32, N, 1.28. $C_{25}H_{14}BrNO_9Os_3$ calcd.: C, 26.74; H, 1.26; N, 1.25%.

Reaction of $Os_3(CO)_{10}(\mu$-Br)(CH=CHPh) with triphenylphosphine

A toluene solution (30 mL) of a mixture of $Os_3(CO)_{10}(\mu$-Br)(CH=CHPh) (120 mg, 0.116 mmol) and 1.5 equiv. of triphenylphosphine (45.6 mg, 0.174 mmol) was heated under reflux for 30 minutes. Then the solvent was removed in a rotary

Table 1

Experimental data for the X-ray diffraction studies of complexes **2** and **3**

	2	**3**
Formula	$C_{25}H_{14}BrNO_9Os_3$	$C_{31}H_{20}BrO_5Os_2P_1$
Molecular weight	1122.9	965.78
Crystal system	monoclinic	triclinic
Space group	$P2_1/c$	$P\bar{1}$
a (Å)	9.977(2)	10.749(2)
b (Å)	22.779(6)	13.101(3)
c (Å)	25.323(5)	13.208(3)
α (°)		118.73(2)
β (°)	95.08(2)	105.49(2)
γ (°)		97.62(2)
U (Å^3)	5732(2)	1495(1)
Z	8	2
D_c (g/cm^3)	2.602	2.145
F(000)	4048	890
Diffractometer	Siemens $R3m/V$	Enraf–Nonius (CAD-4)
Radiation (Å)	λ(Mo-K_α) 0.71073 Å	λ(Mo-K_α) 0.70930 Å
Temperature (K)	296	297
Crystal size (mm)	0.5×0.12×0.10	0.20×0.40×0.50
Scan method	$\theta/2\theta$ scan mode	$\theta/2\theta$ scan mode
2θ (max)	45°	50°
Scan parameter	0.96° + K_α separation	0.65 + 0.35 tan θ
Scan speed (°/min)	2.93 to 14.65	16.48/2 to 16.48/11
h, k, l ranges	0 9, −20 0, −27 27	−12 12, 0 15, −15 3
Absorption correction	psi scan, empirical	psi scan
μ (mm^{-1})	14.72	9.91
Transmission factors max, min	0.989, 0.520	0.4342, 0.9995
Standard reflections	3 measured every 50 reflections	No. 3; variation < 6%, 4 σ; every 3600 seconds
No. of unique data	6800; 4345 with $I \geq 3\sigma(I)$	5298; 4211 with $I > 2\sigma(I)$
No. of atoms and parameters refined	78, 627	60, 362
Mean Δ/σ ratio	0.001	0.004
R; R_w	0.038; 0.037	0.027; 0.026
G.O.F.	1.27	2.36
Residual electron density, e Å^{-3} max/min	1.50/−0.94	1.18/−1.26

Table 2

Atomic coordinates ($\times 10^4$) and equivalent isotropic parameters ($A^2 \times 10^3$) of **2**

	x	*y*	*z*	U_{eq} [a]
Os(1)	1649(1)	4186(1)	4215(1)	41(1)
Os(2)	3658(1)	4902(1)	3720(1)	35(1)
Os(3)	737(1)	4508(1)	3140(1)	42(1)
Os(4)	8504(1)	5805(1)	−475(1)	42(1)
Os(5)	9186(1)	7024(1)	−564(1)	40(1)
Os(6)	6449(1)	6566(1)	−68(1)	39(1)
Br(1)	1646(2)	5573(1)	3356(1)	46(1)
Br(2)	8453(2)	7175(1)	406(1)	48(1)
O(1)	−35(19)	3229(8)	2978(8)	98(9)
O(2)	3129(18)	4080(8)	5314(7)	87(8)
O(3)	5818(16)	4017(7)	4080(6)	70(7)
O(4)	285(18)	4853(9)	1986(7)	94(8)
O(5)	3182(18)	3135(7)	3777(7)	83(8)
O(6)	3722(15)	5434(7)	4819(6)	65(6)
O(7)	256(19)	5335(8)	4490(7)	86(8)
O(8)	−854(19)	3470(8)	4380(8)	93(8)
O(9)	−2052(18)	4831(8)	3494(7)	87(8)
O(1A)	7118(19)	4630(8)	−275(7)	91(8)
O(2A)	9470(18)	8344(7)	−684(7)	83(8)
O(3A)	12126(19)	6736(8)	−147(8)	91(8)
O(4A)	11130(16)	5414(8)	−915(7)	81(8)
O(5A)	9765(17)	6757(7)	−1683(7)	78(7)
O(6A)	4316(18)	5880(7)	−732(7)	78(7)
O(7A)	7036(18)	5917(8)	−1589(6)	83(8)
O(8A)	9942(17)	5872(7)	648(6)	73(7)
O(9A)	6591(21)	5599(8)	782(7)	100(9)
N(1)	5724(21)	5863(9)	3422(7)	63(8)
N(2)	4438(19)	7276(8)	567(7)	58(8)
C(1)	313(22)	3705(12)	3034(9)	64(10)
C(2)	2540(23)	4115(10)	4903(11)	62(10)
C(3)	5005(24)	4361(10)	3934(8)	56(9)
C(4)	410(21)	4725(9)	2427(10)	56(9)
C(5)	2629(26)	3526(11)	3952(8)	60(10)
C(6)	4697(20)	5214(9)	4404(8)	45(8)
C(7)	802(26)	4907(12)	4397(8)	67(10)
C(8)	107(25)	3745(10)	4312(9)	62(10)
C(9)	−1004(26)	4709(10)	3366(8)	57(9)
C(10)	5485(23)	3940(11)	2709(8)	59(10)
C(11)	6670(25)	3767(11)	2476(11)	71(11)
C(12)	7239(25)	4103(14)	2124(11)	80(13)
C(13)	6680(26)	4646(14)	2009(10)	77(12)
C(14)	5565(25)	4809(11)	2222(9)	69(10)
C(15)	4931(20)	4489(9)	2593(7)	40(8)
C(16)	3663(18)	4684(8)	2794(7)	35(5)
C(17)	4967(23)	5506(10)	3505(7)	48(8)
C(18)	6847(33)	6273(13)	3478(14)	111(15)
C(19)	7153(28)	6465(13)	2929(12)	84(8)
C(20)	7671(32)	6129(16)	2595(13)	125(12)
C(21)	8013(37)	6332(18)	2036(16)	149(14)
C(22)	7813(42)	6852(20)	1944(20)	180(18)
C(23)	7492(68)	7238(37)	2383(27)	371(45)
C(24)	6979(75)	6896(33)	2740(28)	417(60)
C(25)	2791(18)	4321(8)	3023(6)	36(7)

Table 2 (continued)

	x	y	z	U_{eq} [a]
C(1A)	7620(24)	5076(10)	−364(8)	53(9)
C(2A)	9373(19)	7849(10)	−643(9)	48(8)
C(3A)	11069(28)	6857(9)	−298(9)	56(9)
C(4A)	10141(26)	5550(9)	−766(8)	50(9)
C(5A)	9528(22)	6862(10)	−1248(10)	60(9)
C(6A)	5105(21)	6139(10)	−486(8)	46(8)
C(7A)	7519(23)	5851(9)	−1178(10)	76(9)
C(8A)	9428(21)	5853(8)	235(8)	42(8)
C(9A)	6581(22)	5955(10)	451(10)	60(9)
C(10A)	4161(22)	7282(11)	−1265(8)	59(9)
C(11A)	2933(24)	7450(10)	−1455(9)	59(10)
C(12A)	2283(22)	7899(10)	−1258(9)	56(9)
C(13A)	2797(23)	8205(9)	−817(10)	56(9)
C(14A)	4070(21)	8037(9)	−597(9)	56(9)
C(15A)	4786(20)	7576(8)	−832(8)	41(8)
C(16A)	6194(21)	7449(8)	−573(7)	45(8)
C(17A)	5167(22)	7030(9)	329(8)	43(8)
C(18A)	3519(26)	7551(10)	863(9)	82(11)
C(24A)	4322(25)	6967(20)	1625(17)	1231(233)
C(19A)	3117	7139	1347	95(9)
C(20A)	1892	6956	1516	576(76)
C(21A)	1872	6600	1964	264(28)
C(22A)	3077	6427	2242	570(69)
C(23A)	4302	6611	2072	1078(209)
C(25A)	7108(8)	7086(7)	−792(7)	36(7)

[a] Equivalent isotropic U_{eq} defined as one third of the trace of the orthogonalized U_{ij} tensor.

evaporator and the residue separated by thin layer chromatography (dichloromethane : hexane = 3 : 1), giving 80 mg of pale yellow $Os_2(CO)_5(PPh_3)(\mu$-Br)(CH=CHPh) (**3**, 0.083 mmol, 72%) and 31 mg of pale yellow $Os_2(CO)_4(PPh_3)_2(\mu$-Br)(CH=CHPh) (**4**, 0.026 mmol, 22%). Crystals of **3** suitable for X-ray diffraction study were obtained by recrystallization from a layered solution of dichloromethane-methanol at room temperature.

Spectral data for **3**: MS (FAB, ^{79}Br, ^{192}Os), *m/z* 968 (M^+). IR (C_6H_{12}): ν(CO), 2072vs, 2012vs, 1993s, 1988s, 1981s, 1950w, 1947m cm^{-1}. ^{1}H NMR (400 MHz, toluene-d_8, 273 K): δ 9.17 (d, 0.42H, J(H–H) = 13.5 Hz); 9.11 (d, 0.58H, J(H–H) = 14.4 Hz); 7.58–6.53 (m, 20H); 4.60 (d, 0.58H, J(H–H) = 14.4 Hz); 4.04 (d, 0.42H, J(H–H) = 13.5 Hz). ^{13}C NMR (100.4 MHz, $CDCl_3$, 266 K): CO, δ 189.7, 184.1, 181.6, 181.2, 179.6, 178.1, 177.1, 174.8, 174.2, 173.5. Elemental analysis: Found: C, 38.56; H, 2.39. $C_{31}H_{22}BrO_5Os_2P$ calcd.: C, 38.55; H, 2.30%.

Spectral data for **4**: MS (FAB, ^{79}Br, ^{192}Os), *m/z* 1202 (M^+). IR (C_6H_{12}): ν(CO), 2021vs, 1988m, 1953s, 1934w cm^{-1}. ^{1}H NMR (400 MHz, $CDCl_3$, 328 K): δ 8.75 (d, 1H, J(H–H) = 13.6 Hz); 7.58–7.10 (br, 30H); 6.97–6.92 (m, 3H); 6.50 (d, 2H, J(H–H) = 6.6 Hz); 3.52 (d, 1H, J(H–H) = 13.6 Hz). ^{13}C NMR (100.4 MHz, $CDCl_3$, 296 K): CO, δ 191.1, 185.9, 182.4, 179.6. Elemental analysis: Found: C, 47.58; H, 3.13. $C_{48}H_{37}BrO_4Os_2P_2$ calcd.: C, 48.04; H, 3.11%.

Reaction of $Os_2(CO)_5(PPh_3)(\mu$-Br)(CH=CHPh) with triphenylphosphine

A toluene solution (30 mL) of a mixture of $Os_2(CO)_5(PPh_3)(\mu$-Br)(CH=CHPh) (39 mg, 0.040 mmol) and two equiv. of triphenylphosphine (21 mg, 0.08 mmol) was heated under reflux in a nitrogen atmosphere. After 35 min, the solvent was evaporated on a rotary evaporator and the residue separated by thin layer chromatography (dichloromethane : hexane = 1 : 3), giving 28 mg of pale yellow $Os_2(CO)_4(PPh_3)_2(\mu$-Br)(CH=CHPh) (0.023 mmol, 58%) as powdery materials.

X-ray crystallography

An orange needle-like single crystal of complex **2** with dimension $0.10 \times 0.12 \times 0.50$ mm^3 was selected and mounted for X-ray analysis. Diffraction measurements were carried out on a Siemens $R3m/V$ diffractometer equipped with graphite-monochromated Mo-K_α radiation. Cell parameters were obtained from a least-squares procedure on 22 reflections with $14.53 < 2\theta < 29.09°$. Systematic absences were identified for $h0l$, $l = 2n + 1$; $0k0$, $k = 2n + 1$. $\theta/2\theta$ scan data were collected at 297 K in the range $0 \leqslant h \leqslant 9$, $-24 \leqslant k \leqslant 0$, $-27 \leqslant l \leqslant 27$ and up to the 2θ limit 45.0°. Corrections for absorption effects were based on ψ-scans of a few suitable reflections with χ values close to 90° (T_{max}, $T_{min} = 0.895$, 0.540, $\mu = 14.72$ cm^{-1}) [8]. No significant variation was observed in intensities of three standards monitored every 50 reflections. 7536 reflections in total were measured, of which 4345 unique structure amplitudes with $I > 3.0\sigma(I)$ were corrected for absorption, Lorentz and polarization effects. The structure was solved by direct methods and refined by full-matrix least-squares based on F values. All non-hydrogen atoms were refined with anisotropic temperature factors. The benzene ring denoted by C19A, C20A, C21A, C22A, C23A and C24A was constrained in the refinement because these atoms showed rather large thermal vibration. All hydrogen atoms were calculated

Table 3

Selected bond distances (Å) and angles (deg) of complex **2** (esd's in parentheses)

(a) Bond distances			
Os(1)–Os(2)	2.948(1)	Os(1)–Os(3)	2.886(1)
Os(1)–C(2)	1.89(3)	Os(1)–C(5)	1.94(2)
Os(1)–C(7)	1.92(3)	Os(1)–C(8)	1.87(3)
Os(2)–C(3)	1.88(2)	Os(2)–C(6)	1.87(2)
Os(3)–C(1)	1.89(3)	Os(3)–C(4)	1.87(3)
Os(3)–C(9)	1.93(3)	Os(3)–C(25)	2.14(2)
Os(2)–C(25)	2.31(2)	Os(2)–C(16)	2.39(2)
Os(2)–C(17)	2.01(2)	Os(2)–Br(1)	2.624(2)
Os(3)–Br(1)	2.630(2)		
(b) Bond angles			
Os(2)–Os(1)–Os(3)	68.2(1)	Os(2)–Br(1)–Os(3)	77.0(1)
Os(1)–C(2)–O(2)	177(2)	Os(1)–C(5)–O(5)	177(2)
Os(1)–C(7)–O(7)	177(2)	Os(1)–C(8)–O((8)	179(2)
Os(2)–C(3)–O(3)	178(2)	Os(2)–C(6)–O(6)	177(2)
Os(3)–C(1)–O(1)	175(2)	O(3)–C(4)–O(4)	177(2)
Os(3)–C(9)–O(9)	179(2)	Os(2)–C(25)–Os(3)	94.5(7)
Os(2)–C(25)–C(16)	77(1)	Os(3)–C(25)–C(16)	126(1)
Os(2)–C(16)–C(25)	70(1)	Os(2)–C(17)–N(1)	175(2)

and refined with fixed U (0.08 Å). At convergence, $R = 0.0378$, $R_w = 0.0368$, $w = [\sigma^2(F) + 0.0004\ F^2]^{-1}$, $\sigma^2(F)$ based on counting statistics, $(\Delta/\sigma)_{max} = 1.266$ (for C24), $S = 1.27$, $(\Delta\rho)_{max} = 1.50$, $(\Delta\rho)_{min} = -0.94$ eÅ^{-3}. Scattering factors were taken from International Tables for X-ray Crystallography, Vol. IV, Kynoch Press, Birmingham, 1974. All calculations were performed on a DEC Micro VAX II computer system using the SHELXTL-PLUS programs (G.M. Sheldrick, SHELXTL-PLUS Crystallographic system, Version 4, Siemens Analytical International Inc., Madison, WI, USA, 1990).

Table 4

Atomic coordinates and equivalent isotropic parameters of complex **3**

	x	y	z	U_{iso}
Os1	0.24509(3)	0.94504(3)	0.27460(3)	3.062(21)
Os2	0.18900(3)	0.74444(3)	0.03239(3)	2.389(18)
Br	0.10269(9)	0.93239(8)	0.07693(7)	3.66(5)
P	0.11468(21)	0.63881(19)	−0.17971(18)	2.82(12)
C1	0.3317(9)	0.9035(8)	0.3865(8)	4.2(6)
C2	0.3339(10)	1.1177(9)	0.3850(8)	4.5(6)
C3	0.0823(10)	0.9373(9)	0.3146(8)	4.4(6)
C4	0.2717(7)	0.6365(8)	0.0576(7)	3.0(5)
C5	0.0331(8)	0.6718(7)	0.0562(7)	3.3(5)
C6	0.3835(7)	0.8921(6)	0.1906(6)	2.8(4)
C7	0.3850(7)	0.8776(7)	0.0769(6)	2.7(4)
C8	0.4905(8)	0.8323(7)	0.0316(7)	3.0(4)
C9	0.5162(8)	0.8486(7)	−0.0594(7)	3.7(5)
C10	0.6153(10)	0.8109(9)	−0.1039(9)	4.8(7)
C11	0.6907(10)	0.7574(9)	−0.0597(10)	5.7(7)
C12	0.6704(9)	0.7372(8)	0.0305(9)	5.2(7)
C13	0.5708(8)	0.7753(8)	0.0743(8)	3.8(6)
C1A	0.1724(8)	0.7265(8)	−0.2429(7)	3.6(5)
C2A	0.1589(9)	0.8409(8)	−0.2005(7)	3.8(5)
C3A	0.2064(10)	0.9101(8)	−0.2440(8)	5.0(6)
C4A	0.2651(11)	0.8613(10)	−0.3303(8)	5.8(7)
C5A	0.2779(12)	0.7477(11)	−0.3738(9)	6.2(8)
C6A	0.2323(9)	0.6771(8)	−0.3308(7)	4.7(6)
C1B	0.1591(9)	0.4995(8)	−0.2537(7)	3.5(5)
C2B	0.2953(9)	0.5033(9)	−0.2053(8)	4.6(6)
C3B	0.3360(11)	0.3995(10)	−0.2553(9)	5.7(8)
C4B	0.2394(14)	0.2902(10)	−0.3554(10)	6.9(9)
C5B	0.1088(12)	0.2855(9)	−0.4042(10)	6.1(8)
C6B	0.0679(9)	0.3879(9)	−0.3556(8)	4.8(6)
C1C	−0.0706(7)	0.5860(7)	−0.2592(6)	2.9(5)
C2C	−0.1336(8)	0.6229(8)	−0.3354(8)	4.4(6)
C3C	−0.2736(11)	0.5813(10)	−0.3911(10)	6.6(8)
C4C	−0.3499(9)	0.5028(10)	−0.3732(9)	5.6(7)
C5C	−0.2865(9)	0.4657(9)	−0.2986(8)	4.9(6)
C6C	−0.1466(9)	0.5063(8)	−0.2408(7)	4.1(6)
O1	0.3811(8)	0.8781(7)	0.4549(6)	7.1(6)
O2	0.3980(8)	1.2181(6)	0.4467(6)	7.0(5)
O3	−0.0097(8)	0.9312(8)	0.3383(7)	7.7(7)
O4	0.3263(6)	0.5711(5)	0.0278(6)	4.6(4)
O5	−0.0532(6)	0.6290(6)	0.0700(5)	5.1(4)

[a] Equivalent isotropic U_{iso} defined as one third of the trace of the orthogonalized U_{ij} tensor.

Table 5

Selected bond distances (Å) and angles (deg) complex **3** (esd's in parentheses)

(a) Bond distances			
Os(1)–Os(2)	2.742(1)	Os(1)–Br	2.563(1)
Hs(2)–Br	2.624(1)	Os(1)–C(1)	1.876(9)
Os(1)–C(2)	1.915(9)	Os(1)–C(3)	1.961(9)
Os(2)–C(4)	1.828(9)	Os(2)–C(5)	1.912(8)
Os(2)–C(7)	2.332(7)	Os(1)–C(6)	2.083(7)
Os(2)–C(6)	2.246(7)	C(6)–C(7)	1.43(1)
C(7)–C(8)	1.48(1)	Os(2)–P	2.390(2)
C(1)–O(1)	1.14(1)	C(2)–O(2)	1.14(1)
C(3)–O(3)	1.12(1)	C(4)–O(4)	1.16(1)
C(5)–O(5)	1.12(1)		
(b) Bond angles			
Os(2)–Os(1)–Br	59.17(3)	Os(1)–Os(2)–Br	57.01(3)
Os(1)–Br–Os(2)	63.83(3)	Os(2)–Os(1)–C(6)	53.4(2)
Os(1)–C(6)–Os(2)	78.5(3)	Os(1)–C(6)–C(7)	128.8(6)
Os(2)–C(6)–C(7)	75.2(4)	Os(2)–C(7)–C(6)	68.6(4)
C(6)–C(7)–C(8)	119.3(7)	Os(2)–Os(1)–C(2)	144.7(3)
Os(1)–Os(2)–P	153.29(5)	Os(1)–C(1)–O(1)	178.2(9)
Os(1)–C(2)–O(2)	172.7(9)	Os(1)–C(3)–O(3)	178.4(9)
Os(2)–C(4)–O(4)	177.1(7)	Os(2)–C(5)–O(5)	175.8(7)

Diffraction measurements on the triphenylphosphine complex **3** were carried out on a Nonius CAD-4 diffractometer. Lattice constants were determined from 25 randomly selected reflections, with 2θ angle in the range 20.82–28.80°. Intensities were corrected for Lorentz, polarization and absorption effects. All data deduction and structural refinement were performed using the NRCC-SDP-VAX packages. The structures were solved by the heavy-atom method and refined by least squares recycle. All non-hydrogen atoms were refined with anisotropic thermal parameters and the hydrogen atoms of the phenyl groups were added at the idealized positions and included in the structure factor calculations.

The data collection and refinement parameters for complexes **2** and **3** are given in Table 1. Atomic positional parameters for complex **2** are found in Table 2, whereas some selected bond angles and lengths are given in Table 3. The corresponding parameters for complex **3** are given in Tables 4 and 5, respectively. Tables of bond distances and angles, tables of positional parameters and anisotropic thermal parameters, and listings of the observed and calculated structural factors are available from the author (Y.C.).

Results and discussion

Reaction with benzyl isonitrile

Treatment of $Os_3(CO)_{10}(\mu\text{-Br})(CH{=}CHPh)$ (**1**) with slight excess of benzyl isonitrile in toluene (85°C, 30 min) induced a CO substitution reaction, giving $Os_3(CO)_9(CNCH_2Ph)(\mu\text{-Br})(CH{=}CHPh)$ (**2**) as the only isolated cluster compound. This complex was separated and purified on silica gel TLC plates, and further characterized by spectroscopic methods. The molecular ion observed in the FAB mass spectra indicates that complex **2** is a triosmium complex with one isonitrile

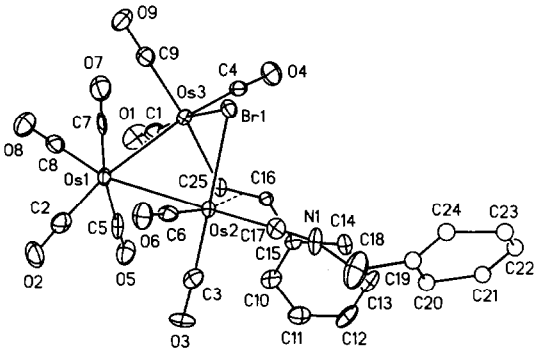

Fig. 1. ORTEP diagram of $Os_3(CO)_9(NCCH_2Ph)(\mu\text{-}Br)(CH{=}CHPh)$ (2).

ligand replacing a CO ligand in complex 1. However, the location of the isonitrile ligand cannot be determined by the spectroscopic techniques, the X-ray diffraction is carried out to establish the structure.

Crystal structure of complex 2

The molecular structure of 2 and the exact location of the isonitrile ligand were determined by single-crystal X-ray diffraction. The ORTEP diagram and the scheme used for labelling the atoms are presented in Fig. 1. The important bond distances and bond angles are summarized in Table 3. The molecule consists of an open triangular arrangement of three osmium atoms with distances Os(1)–Os(2) = 2.948(1), Os(1)–Os(3) = 2.886(1) and Os(2) $\cdots$ Os(3) = 3.270 Å and bond angle Os(2)–Os(1)–Os(3) = 68.2(1)°. Each osmium atom can be considered to possess a pseudo-octahedral geometry and all carbonyl ligands are considered linear. The bromine atom and the ethenyl group bridge the non-bonded osmium atom with distances Os(2)–Br(1) = 2.624(2), Os(3)–Br(1) = 2.629(1), Os(2)–C(25) = 2.31(2), Os(2)–C(16) = 2.39(2) and Os(3)–C(25) = 2.14(2) Å, while the third osmium atom Os(1) is connected to four CO ligands. Thus, the gross molecular geometry and conformation of the ethenyl fragment of 2 resembles those of its precursor 1 and several other triosmium ethenyl derivatives [9]. Furthermore, the isonitrile ligand is coordinated to atom Os(2) and located at an equatorial site which is *trans* to the Os–Os bond and *cis* to the ethenyl carbon–carbon π-bond. The isonitrile and phosphine ligands in the related complexes $H_2Os_3(CO)_9(CN^tBu)$ [10] and $H_2Os_3(CO)_9(P^iPr_3)$ [11] respectively were, similarly, found to occupy the same, less sterically congested, equatorial position.

Reaction with triphenylphosphine

Treatment of $Os_3(CO)_{10}(\mu\text{-}Br)(CH{=}CHPh)$ (1) with 1.5 equivalent of triphenylphosphine in refluxing toluene solution (30 min) produced a dinuclear, monosubstituted $Os_2(CO)_5(PPh_3)(\mu\text{-}Br)(CH{=}CHPh)$ (3) and disubstituted $Os_2(CO)_4(PPh_3)_2(\mu\text{-}Br)(CH{=}CHPh)$ (4) complexes in 72 and 22%, respectively.

When the reaction was repeated with an excess (2.2 equivalent) of triphenylphosphine, we obtained similar results but the yield of 3 was lower (23%) due to its further reaction with triphenylphosphine. Therefore, we propose that the reaction mechanism be considered as a simple phosphine substitution reaction to produce a

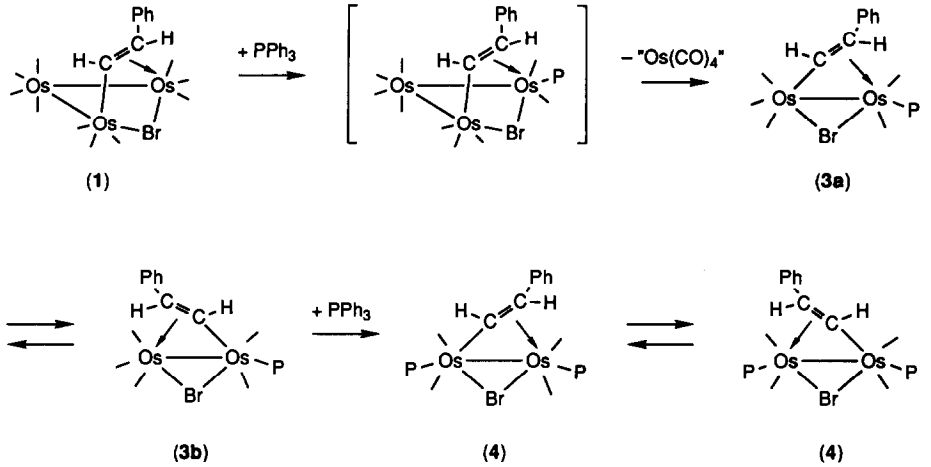

Scheme 1

speculative product $[Os_3(CO)_9(PPh_3)(\mu\text{-}Br)(CH{=}CHPh)]$, followed by elimination of an $Os(CO)_4$ unit to yield the isolated dinuclear complex **3** (Scheme 1). The latter is also an intermediate in the formation of the disubstituted complex **4** because we have confirmed that the reaction of **3** with triphenylphosphine under similar conditions (110 °C, 35 min) generated **4** in 59% yield.

The fragmentation reaction of the intermediate $Os_3(CO)_9(PPh_3)(\mu\text{-}Br)(CH{=}CHPh)$ is in contrast to the reactivity of a related complex $Os_3(CO)_9(PPh_2Et)(\mu\text{-}H)(CH{=}CH_2)$ [12]. On thermolysis, this hydrido complex failed to fragment but instead elminated CO to afford a vinylidene complex $Os_3(CO)_8(PPh_2Et)(\mu\text{-}H)_2(C{=}CH_2)$. We propose that the difference in reactivity is due to the presence of relatively weak Os–Os bonding interactions in **1** or in the postulated intermediate $Os_3(CO)_9(PPh_3)(\mu\text{-}Br)(CH{=}CHPh)$. The weakening of the Os–Os interaction can be rationalized by a *cis*-labilization effect, as observed in mononuclear transition metal complexes [13]. There have been reports [14,15] that a bridging chloride atom or the oxygen atom of the bridging acyl group enhances site selectivity and rate of CO substitution on the adjacent transition metal centres. For a similar reason, it is highly possible that the bridging bromide atom in our system facilitates the cleavage of the nearby Os–Os bonds.

Crystal structure of complex 3

The structure of **3** was also determined by single crystal X-ray diffraction. The ORTEP diagram is displayed in Fig. 2 and the important bond distances and the bond angles are listed in Table 5. The molecule consists of one $Os(CO)_3$ unit and one $Os(CO)_2(PPh_3)$ unit linked by a single Os–Os bond, a bridging bromine atom and a bridging ethenyl group. Again, each osmium atom is considered to be located at the center of a pseudo-octahedron. All the carbonyl ligands are linear, with the average Os–CO angle being 176.4°. The Os(1)–Os(2) distance 2.742(1) Å is shorter than the nonbonding Os · · · Os distance (3.277(2) Å) found in the parent complex 1 and is slightly shorter than the average Os–Os distance (2.877 Å) in $Os_3(CO)_{12}$ [16].

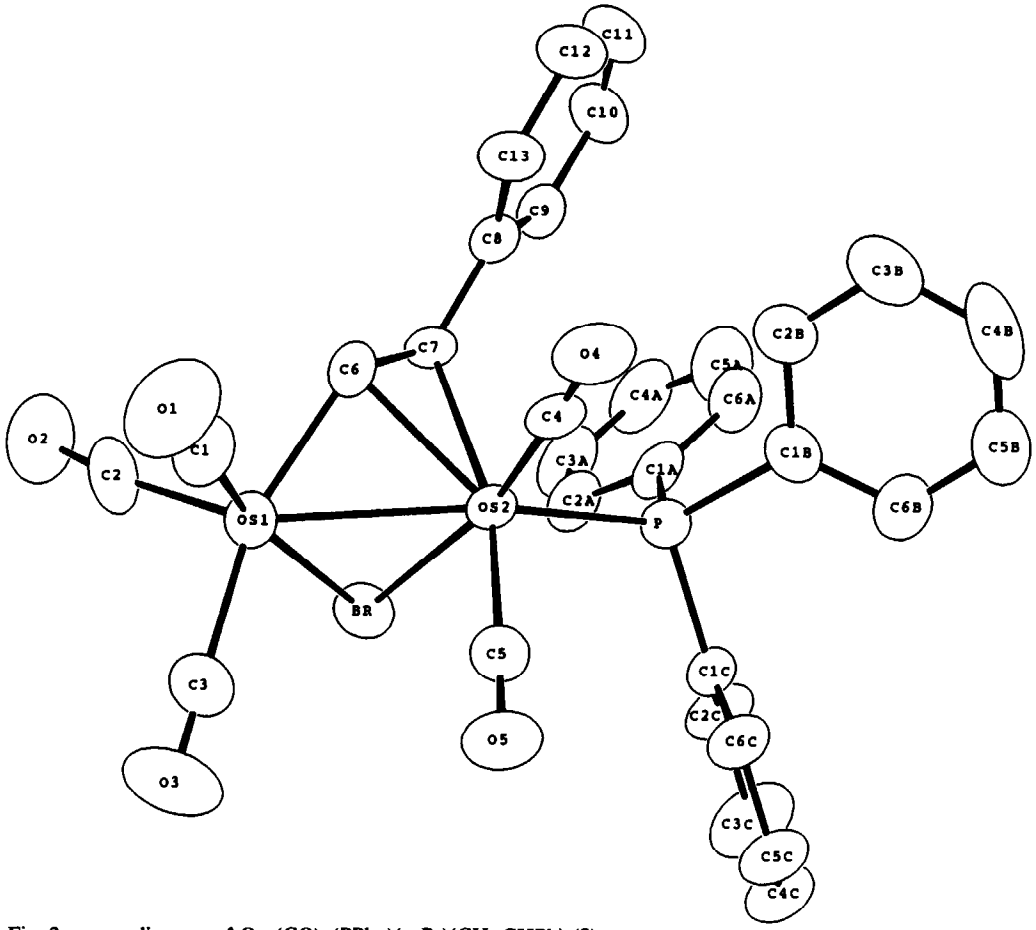

Fig. 2. ORTEP diagram of $Os_2(CO)_5(PPh_3)(\mu\text{-}Br)(CH{=}CHPh)$ (3).

The phosphine ligand occupies a transoid position to the Os–Os vector, with bond distance Os(2)–P = 2.390(2) Å and bond angle Os(1)–Os(2)–P = 153.29(5)°. That the observed bond angle deviates from linearity indicates that the phosphine is bent slightly towards the bridging bromine atom thus minimizing the steric interaction with the adjacent CO ligands. The bridging bromine ligand is connected to both osmium atoms, with bond distances Os(1)–Br = 2.563(1) and Os(2)–Br = 2.624(1) Å and angle Os(1)–Br–Os(2) = 63.83(3)°. The difference between these two Os–Br bonds suggests that the bromo ligand functions as a two-electron donor to the Os(1) atom but as a one-electron donor to Os(2). This asymmetric bonding interaction has been observed with other bridging heteroatoms such as halide, thiolate and phosphido fragments [17]. Finally, the phenyl ethenyl group (C=CHPh) is σ-bonded to atom Os(1) with Os(1)–C(6) = 2.083(7) Å and π-bonded to Os(2) atom with Os(2)–C(7) = 2.332(7) and Os(2)–C(6) = 2.246(7) Å. The bonding resembles the typical μ_2-η^2 bonding mode described for several related dinuclear [18] and trinuclear ethenyl complexes [9].

Solution dynamics of complexes 3 and 4

The ^{1}H NMR spectrum of the isonitrile substituted derivative **2** in $CDCl_3$ at 294K exhibits two doublets at δ 6.99 and 5.92 with coupling constant J(H–H) = 16.0 Hz, in addition to proton signals of the two phenyl substituents and a pseudo-quartet for the methylene fragment of the isonitrile ligand. While the temperature was decreased to 180 K in CD_2Cl_2, its ^{1}H NMR spectrum remained the same, suggesting that there is only one isomer in solution. On the other hand, when a toluene-d_8 solution of **2** was heated in a NMR tube at 98°C for 45 min, we observed virtually no change of the ^{1}H NMR spectrum but the appearance of some unidentified, broad signals due to decomposition. These results strongly indicate that the structure of **2** in solution is identical to its solid state structure and that the ethenyl $\pi \rightarrow \sigma, \sigma \rightarrow \pi$ rearrangement is prohibited under the conditions.

The solution dynamics of the dinuclear phosphine complexes **3** and **4** were completely different. The first indication of the existence of two isomers of complex **3** in solution was in the IR ν(CO) spectrum which shows seven, distinct terminal CO stretching bands. In addition, the ^{1}H NMR spectrum at 273 K in toluene-d_8 displayed one pair of doublet signals at δ 9.17 and 4.04 with coupling constant J(H–H) = 13.5 Hz and a second pair of doublets at δ 9.11 and 4.60 with coupling constant J(H–H) = 14.4 Hz, in addition to the complex signals due to the protons of the phenyl group (Fig. 3). These four doublets are assigned to the *trans*-hydrogens of the ethenyl fragment (CH=CHPh) and, therefore, their relative abundance (1 : 1 : 1.38 : 1.38) indicates that the relative ratio of the isomers is 1 : 1.38. On warming to 305K, the two downfield doublet signals at δ 9.17 and 9.11 broadened and coalesced to give a broad signal at δ 9.08; at 329 K, the two highfield doublets at δ 4.60 and 4.04 also coalesced to a very broad signal at δ 4.55. The fast exchange limiting spectrum was recorded at 375 K, in which we observe two sharp, doublet signals at δ 9.01 and 4.62 with a coupling constant J(H–H) = 14 Hz. We propose that the observed behaviour is due to a rapid $\pi \rightarrow \sigma, \sigma \rightarrow \pi$ rearrangement of the ethenyl ligand (Scheme 1). From the chemical shift difference of the two highfield doublets (224 Hz) and the coalescence temperature (T_c = 329 K), we calculate the free energy of activation $\Delta G^{\ddagger}$ = 64 kJ/mol.

The ^{13}C NMR spectrum of a ^{13}CO enriched sample of **3** was recorded at 266 K in

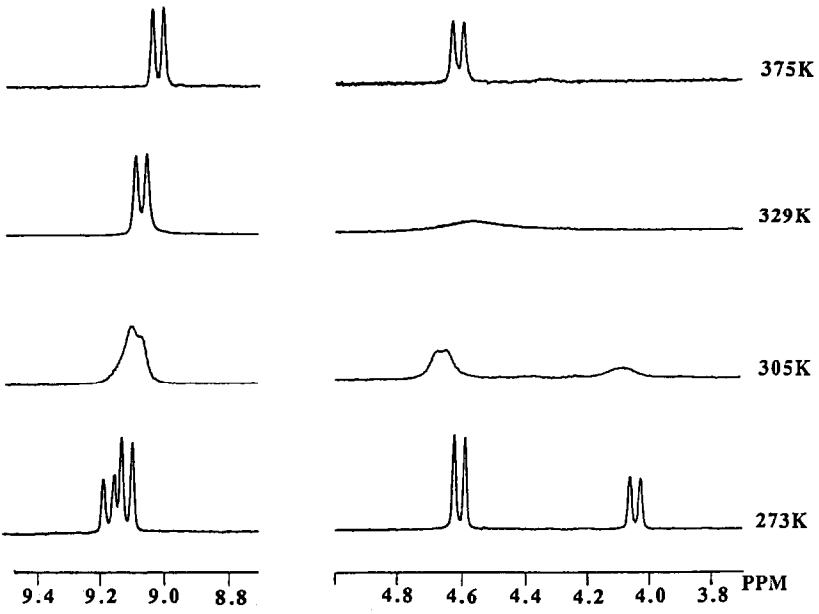

Fig. 3. Variable temperature ^{1}H NMR spectra (toluene-d_8) of 3, showing the region of ethenyl proton signals.

toluene-d_8, showing ten CO signals at δ 189.7, 184.1, 181.6, 181.2, 179.6, 178.1, 177.1, 174.8, 174.2 and 173.5 in the ratios 1.38 : 1 : 1 : 1.38 : 1.38 : 1 : 1 : 1.38 : 1.38 : 1 (Fig. 4). The exact assignment is difficult to achieve, but we can sort these ten signals into two groups based on their intensities and on the existence of two exchanging isomers. On warming to 373 K, these signals broadened and merged to

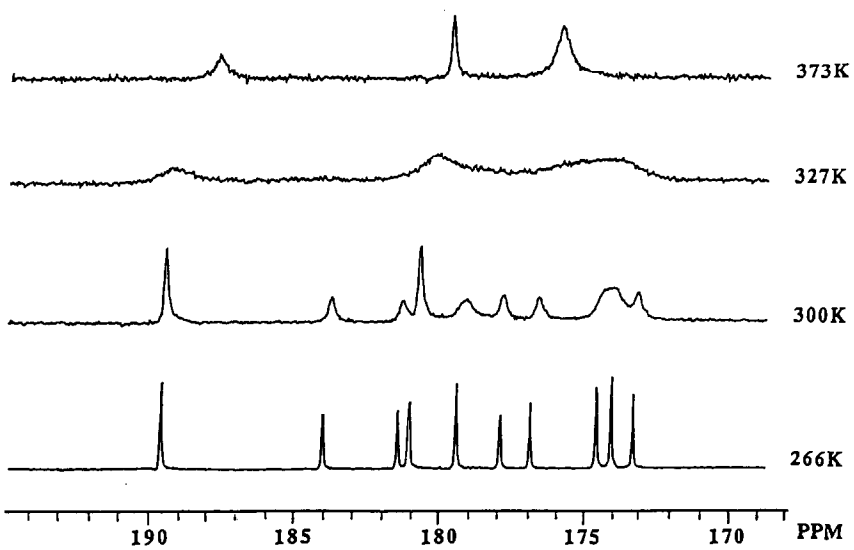

Fig. 4. Variable temperature ^{13}C NMR spectra of 3 in $CDCl_3$ solution, showing the region of CO resonances. The spectrum at 373 K was recorded with toluene-d_8 as solvent.

three broad signals at δ 186.8, 178.8 and 175.1 with relative intensity 1 : 1 : 3. The first two signals at δ 186.8 and 178.8 are assigned to the CO ligands of the $Os(CO)_2(PPh_3)$ unit and the signal at δ 175.1 is assigned to the three CO ligands of the $Os(CO)_3$ unit. This observed pattern indicates that, although the $\pi \rightarrow \sigma, \sigma \rightarrow \pi$ rearrangement of the ethenyl group and the localized threefold rotation of the $Os(CO)_3$ unit are fairly rapid under these conditions, the pairwise exchange of the CO ligands of the $Os(CO)_2(PPh_3)$ unit is either slow or nonexistent. This observation is in contrast to a previous report [19], which has shown that the threefold rotation of $M(CO)_2(PR_3)$ and $M(CO)_3$ groups has similar activation energies. Finally, and most important, this deduction is the key evidence for the rationale for the flipping of the ethenyl group in the related diosmium complex **4**.

The ^1H NMR spectrum of **4** in $CDCl_3$ shows the expected doublet signals of the ethenyl group at δ 8.75 and 6.50 with coupling constant $J(H-H) = 13.6$ Hz and the signals due to the protons of the phenyl groups. However because the structure of **4** consists of two identical $Os(CO)_2(PPh_3)$ metal units and because the rearrangement of the ethenyl group would only generate an enantiomer, the rearrangement of the ethenyl group would not affect the appearance of the signals of the ethenyl doublets in ^1H NMR spectroscopy.

We circumvented the above problem by using ^{13}C NMR spectroscopy instead. The ^{13}C NMR spectrum of a ^{13}CO enriched sample of **4** in toluene-d_8 at 310 K exhibits four CO signals at δ 191.7, 186.4, 182.8 and 180.2. When the temperature was increased, we observed that the signals at δ 182.8 and 180.2 broadened and coalesced to form a signal at δ 181.3 and 330 K and the signals at δ 191.7 and 186.4 gave a broad signal at δ 188.7 and 354 K. Finally, the spectrum displayed one broad signal at δ 187.3 and one relatively sharp signal at δ 181.1 at 380 K.

The observed exchange behaviour can be understood in terms of two completely different types of ligand movement. The first type involves two localized pairwise exchanges of the CO ligands on the different $Os(CO)_2(PPh_3)$ unit. This hypothetical motion would average the environment of the CO pair on the same metal atom and give two signals because there are two non-equivalent $Os(CO)_2(PPh_3)$ units in the molecule. The second one involves the $\pi \rightarrow \sigma, \sigma \rightarrow \pi$ rearrangement of the ethenyl group. This process would create a time-averaged mirror plane which is perpendicular to and bisects the Os–Os bond; therefore, the $Os(CO)_2(PPh_3)$ units become equivalent under this condition. We expect to see two CO signals if there were no pairwise exchange on the $Os(CO)_2(PPh_3)$ units.

We eliminate the first possibility by means of the argument developed earlier, in which we concluded that the pairwise exchange of the CO ligand is much slower than the $\pi \rightarrow \sigma, \sigma \rightarrow \pi$ rearrangement of the ethenyl group. In agreement with our proposal, the free energy of activation ($\Delta G^{\ddagger} = 66$ kJ/mol), calculated from the chemical shift difference of the ^{13}CO signals at δ 191.7 and 186.4 (533 Hz) and the coalescence temperature ($T_c = 354$ K), is also similar to that of complex **3**.

Summary

We have shown that the reaction of the triosmium ethenyl complex **1** with benzyl isonitrile gives a simple substitution product. In contrast, reaction with triphenylphosphine, inducing cluster fragmentation, yields phosphine substituted diosmium derivatives. These ligand substitution reactions are very sensitive to the properties of the nucleophile as is shown by the outcome of the reaction with triphenylphosphine

being so different from that of the reaction with methyldiphenylphosphine. When the complex was reacted with the stoichiometric amount of methyldiphenylphosphine in toluene solution (90 °C, 50 min), we failed to detect either the formation of CO substitution or any cluster fragmentation other than decomposition.

Furthermore, the successful isolation of these derivatives allowed us to study the fluxional motion of the bridging μ_2-η^2-ethenyl group. Our results indicate that the ethenyl group of the benzyl isonitrile derivative **2** is static at least on the time scale of ^{1}H NMR spectroscopy. However, variable temperature ^{1}H and ^{13}C NMR studies indicated that the ethenyl group of triphenylphosphine substituted derivatives **3** and **4** in solution undergoes rapid $\pi \rightarrow \sigma, \sigma \rightarrow \pi$ rearrangement.

Acknowledgments

We are grateful to the Refining & Manufacturing Research Center of the Chinese Petroleum Corporation (Republic of China) for financial support.

References

1 (a) J.F. Knifton, J. Am. Chem. Soc., 103 (1981) 3959; (b) P.C. Ford and A. Rokicki, Adv. Organomet. Chem., 28 (1888) 139.
2 (a) B.D. Dombek, Organometallics, 4 (1985) 1707 and references therein; (b) G. Ertl, M. Weiss and S.B. Lee, Chem. Phys. Lett., 60 (1979) 391; (c) G. Broden, G. Gafner and H.P. Bonzel, Surf. Sci., 84 (1979) 295.
3 E.D. Morrison and G.L. Geoffroy, J. Am. Chem. Soc., 107 (1985) 3541.
4 S. Rivomanana, G. Lavigne, N. Lugan, J.-J. Bonnet, R. Yanez and R. Mathieu, J. Am. Chem. Soc., 111 (1989) 8959.
5 K.-L. Lu, J.-L. Chen, Y.-C. Lin and S.-M. Peng, Inorg. Chem., 27 (1988) 1726.
6 Y. Chi, B.-F. Chen, S.-L. Wang, R.-K. Chiang and L.-S. Hwang, J. Organomet. Chem., 377 (1989) C59.
7 (a) J.R. Shapley, S.I. Richter, M. Tachikawa and J.B. Keister, J. Organomet. Chem., 94 (1975) C43; (b) A.A. Koridze, O.A. Kizas, P.V Petrovskii, N.E. Kolobova, Yu.T. Struchkov and A.I. Yanovsky, ibid., 338 (1988) 81.
8 N.W. Alcock, Acta Crystallogr., Sect. A, 30 (1974) 332.
9 (a) E. Sappa, A. Tiripicchio and A.M.M. Lanfredi, J. Organomet. Chem., 249 (1983) 391; (b) J.J. Guy, B.E. Reichert and G.M. Sheldrich, Acta Crystallogr., Sect. B, 32 (1976) 3319; (c) E. Boyar, A.J. Deeming, K. Henrick, M. MacPartlin and A. Scott, J. Chem. Soc., Dalton Trans., (1986) 1431; (d) A.D. Clauss, M. Tachikawa, J.R. Shapley and C.G. Pierpoint, Inorg. Chem., 20 (1981) 1528.
10 (a) R.D. Adams and N.M. Golembeski, Inorg. Chem., 18 (1979) 1909; (b) R.D. Adams and N.M. Golembeski, J. Am. Chem. Soc., 101 (1979) 2579.
11 L.J. Farrugia, J. Organomet. Chem., 394 (1990) 515.
12 C.B. Simon and J. Evans, J. Chem. Soc., Dalton Trans., (1982), 1049.
13 D.F. Lichtenberger and T.L. Brown, J. Am. Chem. Soc., 100 (1978) 366 and references therein.
14 Y. Chi, J.R. Shapley, J.W. Ziller and M.R. Churchill, Organometallics, 6 (1987) 301.
15 (a) A. Mayr, Y.C. Lin, N.M. Boag, C.E. Kampe, C.B. Knobler and H.D. Kaesz, Inorg. Chem., 23 (1984) 4640; (b) C.E. Kampe and H.D. Kaesz, ibid., 23 (19840 4646.
16 M.R. Churchill and B.G. de Boer, Inorg. Chem., 16 (1977) 878.
17 (a) R. Yanez, J. Ros, R. Mathieu, X. Solans and M. Font-Bardia, J. Organomet. Chem., 389 (1990) 219.
18 (a) J.A. Iggo, M.J. Mays, P.R. Raithby and K. Henrick, J. Chem. Soc., Dalton Trans., (1983) 205; (b) J. Ros, J.M. Vinas, R. Mathieu, X. Solans and M. Font-Bardia, J. Organomet. Chem., 307 (1986) C7; (c) J. Ros, J.M. Vinas, R. Mathieu, X. Solans and M. Font-Bardia, J. Chem. Soc., Dalton Trans., (1988) 281; (d) I. Moldes, J. Ros, R. Yanez, R. Mathieu, X. Solans and M. Font-Bardia, J. Organomet. Chem., 395 (1990) 305.
19 E. Rosenberg, C. Barner-Thorsen, L. Milone and S. Aime, Inorg. Chem., 24 (1985) 231.